Continental Shelf Research 211 (2020) 104288

Contents lists available at ScienceDirect

Continental Shelf Research

journal homepage: http://www.elsevier.com/locate/csr

A new approach to analytical modelling of groyne fields

Antonios Valsamidis [a], Dominic E. Reeve [a,*]

[a] Zienkiewicz Centre for Computational Engineering, College of Engineering, Swansea University, Fabian Way, Swansea, SA1 8EN, UK

ARTICLE INFO

Keywords:
Groyne
Groyne-field
Shoreline evolution
Erosion
Coastal defence scheme

ABSTRACT

Analytical and computational techniques for finding solutions to the equations describing shoreline evolution are widely known and the advantages and disadvantages of both are well documented. Initial analytical solutions to the 1-line models were restricted to constant wave conditions and simple beach/structure configurations. Recent developments in analytical treatments have allowed solutions to be found for an arbitrary sequence of wave conditions, but again for simple configurations. Here, we propose a method of linking several analytical solutions together in order to describe the unsteady evolution of a beach within a groyne field, allowing for both permability of the groynes and by-passing. The method relies on specifying boundary conditions in each groyne cell that mimic the transmission and by-passing of sediment. The conditions are generalisations of boundary conditions that are well-known. Solutions for groyne fields on straight and convex shorelines are presented to illustrate the method for constant and time varying wave conditions.

1. Introduction

1.1. Background

Groynes are elongated coastal structures placed normal to the shore. They are usually made of timber, concrete or rock and their purpose is to interrupt the wave-driven longshore transport of sand along the beach in order to mitigate erosion. However, given a predominant longshore drift, accretion is expected on the updrift side of the groyne and erosion on the downdrift side, due to the blockage of longshore sediment transport by the groyne. Thus the application of groynes as a means of coastal protection is only partly effective as every area of accretion is balanced by a corresponding area of erosion. Extremes of accretion and erosion can be avoided by placing a sequence of groynes along a stretch of beach between two control points such as headlands which place a natural limit on the movement of sand. Alternatively, on a long open stretch of beach groyne fields might be constructed to taper the amount of sediment retained by the groynes near the edge of the groyne field. In this case, reducing the length of the groyne promotes bypassing of sand around the seaward tip, reducing the height allows sediment in suspension to overtop the groyne and increasing the permeability allows the transmission of sediment through the trunk of the groyne, as illustrated in Fig. 1.

It is, as a result, not uncommon to see series of groynes along a beach. Such an arrangement is called a groyne field; and example is shown in Fig. 2.

A groyne field must be carefully designed to maintain the sediment material in the beach fronting the area being protected. Specifically, if the groyne length is too short sediment bypassing at the tips of the groynes may occur to an excessive degree resulting in poor sediment retention, (Coghlan et al., 2013). If the groynes are too long or too high or impermeable (e.g. mass concrete), an inadequate amount of sediment flow may pass to their downdrift side, and consequently, the sediment material which has already been lost in this area will not be replaced causing erosion downdrift of the groynes, (Hanson et al., 2008).

Terminal groyne syndrome refers to the erosion which is expected to occur downdrift of the terminal groyne in a groyne field. Examples of extreme negative impacts of this phenomenon include Southwick beach in West Sussex, UK, as shown in Fig. 3a, (Clarke et al., 2017), as well as Westhampton beach in New York, shown in Fig. 3b, (Dean and Dalrymple, 2002) (see Fig. 4).

Further details of principles governing groyne design may be found in Fleming (1990), Kraus et al. (1994), Basco and Pope (2004). Here, our focus is on techniques to assist in predicting how a beach will respond to the construction of a groyne field.

1.2. Beach model background

The One-Line model, a simplified physics-based model, is generally used for simulating medium to long-term shoreline morphodynamic

* Corresponding author.
E-mail address: d.e.reeve@swansea.ac.uk (D.E. Reeve).

https://doi.org/10.1016/j.csr.2020.104288
Received 23 October 2019; Received in revised form 26 June 2020; Accepted 25 October 2020
Available online 28 October 2020

evolution, on shorefronts extending up to approximately 30 km, (Gravens et al., 1991). The One-Line model has successfully served over time as a robust and reliable tool for assessing beach morphodynamic evolution, (e.g. US Army Corps, 2002), and is considered a suitable tool for testing the performance of groyne-fields for certain wave and hydrodynamic conditions with respect to specific beaches, and for a variety of different geometric parameters as far as the groyne length, groyne permeability and groyne spacing is concerned.

The One-Line model is based on a combination of the continuity of mass equation and a longshore sediment transport equation (e.g. Larson et al., 1987). The primary assumptions are: (a) the beach profile is in equilibrium and is unchanging in time, (this implies the bathymetric contours are parallel to each other so that one contour is sufficient to predict the entire beach movement; (b) The longshore sediment transport takes place up to a specific depth, the depth of closure D_c. No longshore sediment transport is considered to occur seaward of this.

Early analytical solutions to the One-Line Model were based on the assumption of constant wave forcing, mild shoreline gradient and small wave angle with respect to the shoreline orientation. With these restrictions the equations may be condensed into a single diffusion-type equation (Eq. (1)), (Pelnard-Considère,1956):

$$\frac{\partial y}{\partial t} = \varepsilon \frac{\partial^2 y}{\partial x^2} \tag{1}$$

where x is the longshore distance on an axis X parallel to the shoreline trend, y is the shoreline position on a Y axis vertical to X, ε is the diffusion coefficient, and t is time.

Computational integration of the one-line model is based on the simultaneous solution of three equations: continuity; longshore transport; and a geometrical expression relating the wave and beach angles. Time varying wave conditions, larger wave angles and nearshore wave transformation such as diffraction can be incorporated into computational schemes to enhance their general applicability, (see e.g. Gravens et al., 1991; Hanson, 1989; Hanson and Kraus, 1989). They have been used to investigate the evolution of more complex situations such as groyne fields, and for design purposes.

The one-line framework can also be extended to include one or more additional contours in order to provide a better description of the cross-shore variation in the dynamics. Nevertheless, the cross-shore exchange of sediment between the contours is usually parameterised in the form of a relaxation towards an equilibrium shape. Two-line models, in the form of the analytical approach of Bakker (1969) and the computational solution of Horikawa et al. (1979) provided the simplest description of changes in beach slope, while the multi-line, (or N-line), models proposed by Perlin and Dean (1979, 1983) and Steetzel et al. (1988) provided additional fidelity to the description of cross-shore transport dynamics. However, N-line models have yet to find wide acceptance and usage in practice. This has been attributed to the greater data demands they make and, to a lesser extent, the longer computing time they require. Another reason may be their susceptibility to numerical instability noted by Perlin and Dean (1983) and Shibutani et al. (2009). Their inherent instability under certain conditions was subsequently established by Reeve and Valsamidis (2014) for small wave and shoreline angles.

On the other hand, analytical solutions to the One-Line model can be utilized for isolating and remotely studying specific coastal phenomena, and consequently validating testing computational models, (Hanson, 1987; Wind, 1990; Walton, 1994). Further, analytical solutions can be evaluated immediately for any chosen time, rather than timestepping over many small intervals as in computational approaches. With additional efforts, researchers have loosened some of the fundamental restrictions of analytical solutions. For instance, Larson et al. (1997) produced an analytical solution to the One-Line Model, via Laplace transform techniques, for a single groyne and a groyne-compartment, assuming sinusoidally time-varying wave angle. An approximate method for allowing arbitrary time varying conditions was proposed by Walton and Dean (2011) and Valsamidis et al. (2013). This combined previous analytical solutions for constant wave conditions with a Heaviside scheme to allow a solution for arbitrarily varying wave time-series to be constructed. The same approach was adopted by Valsamidis and Reeve (2017) to develop solutions for the case of a beach with a groyne and a river-mouth, with the latter acting as a source or sink of sediment discharge influencing the shoreline evolution near the groyne.

Analytical solutions to Eq. (1) produced via Fourier transform techniques can include time-varying wave conditions without needing modifications such as the application of a Heaviside scheme to do so. Reeve (2006) presented an analytical solution, based on Fourier transform techniques, for the case of an impermeable groyne on an arbitrary initial shoreline shape subject to arbitrarily varying wave conditions. The solution was presented in the form of integrals that required numerical evaluation to capture the effect of arbitrary wave conditions. Such kinds of solutions have been termed ‘semi-analytical’ because although they are derived analytically, they require numerical integration for their evaluation. In this paper we extend the range of applicability of semi-analytical solutions by proposing new boundary conditions that mimic by-passing around the groyne tip and groyne permeability, as well as extending solutions to describe a groyne field.

2. Methodology

The strategy is to combine semi-analytical solutions for a single

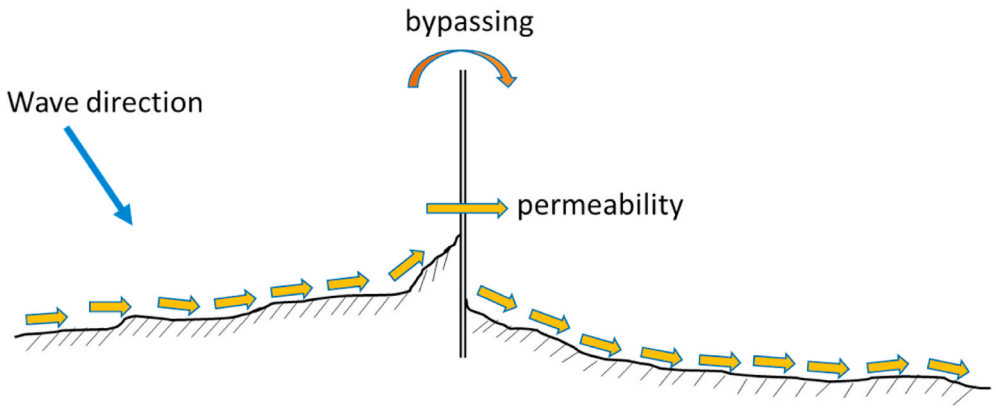

Fig. 1. For a specific direction of the littoral drift (shown by the orange arrows along the beach), accretion is caused on the updrift side of the groyne (denoted by the vertical double line) and erosion downdrift-wards. Sediment material is illustrated to pass through the body of the groyne, and to bypass its tip. (For interpretation of the references to colour in this figure legend, the reader is referred to the Web version of this article.)

groyne and a groyne compartment to form a model suitable for describing an extended groyne field. Specifically, the semi-analytical solution regarding shoreline evolution near a groyne (Reeve, 2006) was coupled with the one derived by Zacharioudaki and Reeve (2008) for a groyne compartment, with an appropriate internal boundary condition.

2.1. The semi-analytical solution for shoreline evolution near a groyne

Reeve (2006) used a Fourier cosine transform to develop a solution to Eq. (1) for arbitrary initial beach shape and wave conditions for shoreline evolution near a groyne.

This solution consists of the sum of the following 3 terms:

$$y_1^G = \frac{1}{\pi}\left(\pi\int_0^t \varepsilon(u)du\right)^{-1/2}\int_0^{+\infty} g(\xi)\left[\exp\left(-\frac{(x-\xi)^2}{4\int_0^t \varepsilon(u)du}\right)+\exp\left(-\frac{(x+\xi)^2}{4\int_0^t \varepsilon(u)du}\right)\right]d\xi \quad (2)$$

where $g(x)$ is the initial shoreline position, and ξ is a dummy variable used in the integration process. In many cases the initial beach is taken as a straight line with $g(x) = 0$ in which case this term is identically zero. y_1^G describes the contribution of the initial shoreline shape to the consequent evolution;

$$y_2^G = \frac{2}{\pi}\int_0^{+\infty}\left(\int_0^t \exp\left(-\int_w^t \left[\omega^2\varepsilon(u)\right]du\right)\tilde{q}(\omega,w)dw\right)\cos(\omega x)d\omega \quad (3)$$

where ω is the transform variable used in the Fourier cosine transform operation, $\tilde{q}$ is the Fourier cosine transformed variable of q; the latter parameter describes the sediment flow from a source or sink of sediment discharge, and w is a variable related to time. Again, in case that there are no sources or sinks $q(t)$ may be considered equal to zero, and the second term is zero as well. This term corresponds to the impact of a source or sink of sediment discharge on shoreline evolution;

$$y_3^G = \frac{1}{\sqrt{\pi}}\int_0^t \varepsilon(w)j(w)\left(\frac{1}{\sqrt{\pi\int_w^t \varepsilon(u)du}}\exp\left(-\frac{x^2}{4\int_w^t \varepsilon(u)du}\right)\right)dw \quad (4)$$

where $j(w)$ is the boundary condition at the groyne. The third term y_3^G corresponds to the impact of the combination of wave action and the boundary condition at the groyne on the shoreline evolution. If the time variation of $\varepsilon(t)$ has a specified functional form, the integration of Eq. (4) may be performed analytically. Alternatively, if $\varepsilon(t)$ is specified by an arbitrary time-series then the integrals must be evaluated numerically.

Finally, the shoreline position is given as the summation of Eqs. (2)–(4):

$$y^G = y_1{}^G + y_2{}^G + y_3{}^G \quad (5)$$

The semi-analytical solution has been tested, for a range of simple conditions, against analytical solutions by Valsamidis (2016) and Valsamidis and Reeve (2017).

2.2. The semi-analytical solution for a groyne compartment

Zacharioudaki and Reeve (2008) provided a semi-analytical solution to the One-Line model for the case of shoreline evolution in a groyne compartment (Fig. 5):

The shoreline evolution in a groyne compartment is described by a solution to Eq. (1), which is derived via finite Fourier cosine transforms. This solution comprises of the following 4 terms:

$$y_1^{GC} = \frac{1}{a}\bar{g}(0) + \frac{1}{a}\int_0^t \varepsilon(w)(j(w)-k(w)+\hat{s}(0,w))dw \quad (6)$$

$$y_2^{GC} = \frac{2}{a}\sum_{\psi=1}^{+\infty}\cos\left(\frac{\psi\pi x}{a}\right)\hat{g}(\psi)\exp\left(-\int_0^t \frac{\pi^2\psi^2}{a^2}\varepsilon(u)du\right) \quad (7)$$

$$y_3^{GC} = \frac{2}{a}\sum_{\psi=1}^{+\infty} cos\left(\frac{\psi\pi x}{a}\right)\int_0^t \exp\left(-\int_w^t \varepsilon(u)\left(\frac{\psi\pi}{a}\right)^2 du\right)\left(\varepsilon(u)((-1)^{\psi}j(w)-k(w))dw\right) \quad (8)$$

$$y_4^{GC} = \frac{2}{a}\sum_{\psi=1}^{+\infty} cos\left(\frac{\psi\pi x}{a}\right)\int_0^t \exp\left(-\int_w^t \varepsilon(u)\left(\frac{\psi\pi}{a}\right)^2 du\right)\hat{s}(\psi,w)dw \quad (9)$$

In the above equations $g(x)$ corresponds to the initial shoreline position, $\hat{g}(\psi) = \int_0^a g(x)cos\left(\frac{\psi\pi x}{a}\right)dx$ thus, $\hat{g}(0) = \int_0^a g(x)dx$; 'a' refers to the groyne compartment's length; $\hat{g}(\psi)$ is the finite-Fourier cosine transform of $g(x)$; ψ is an integer transform variable; $j(w)$ is the time-varying

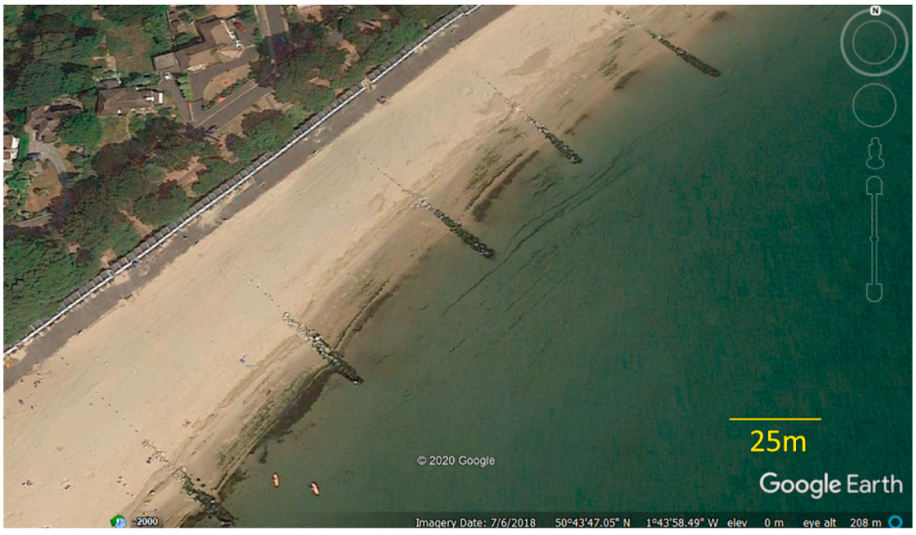

Fig. 2. Groyne field in Mudeford, England (extracted from Google Earth).

boundary condition on the left side of the groyne compartment; *k(w)* is the corresponding boundary condition on the right side of the groyne compartment; *w* is a dummy variable of integration running from time *0* to arbitrary time *t*. The integrals with respect to *u* yield a number for a given value of *t* while those with respect to *w* require numerical evaluation. Finally, the source term appearing in Eq. (6) is given by:

$$\hat{s}(0,w) = \int_0^a s(x,w)dx$$

The term y_2^{GC} incorporates the initial shoreline shape while y_3^{GC} the boundary conditions at the groynes. The source term is described by the fourth term y_4^{GC}. However, the term y_1^{GC} involves the initial shoreline position, the source term and the boundary conditions. Finally, the shoreline evolution in a groyne compartment is given by the summation of Eqs. (6)–(9):

$$y^{GC} = y_1{}^{GC} + y_2{}^{GC} + y_3{}^{GC} + y_4{}^{GC} \quad (10)$$

where *j(w)* and *k(w)* are the boundary conditions on the left-hand side and right-hand side groynes of the groyne compartment, respectively.

2.3. A new internal boundary condition for combining different solutions

A groyne field can be considered as the concatenation of single groynes and groyne compartments. The solutions for these cases may be combined to give a solution for a groyne field as shown in (Fig. 6):

Thus, a groyne field might be modelled for a chosen number of groynes, with the option to consider open external boundaries, and as initial condition, an arbitrary shoreline shape (Fig. 7):

Early analytical solutions treated the case of impermeable groynes of infinite length. Here we seek an internal boundary condition that reflects real life more closely. That is, a condition that allows sediment transport to take place through and around groynes. In other words, a condition that mimics groynes of finite length that are permeable with the potential of sediment bypassing around their seaward tip. Hanson (1989) proposed the following formula for describing the portion of longshore sediment flux *ra* that bypasses a groyne (Eq. (10)):

$$ra = 1 - \frac{D_G}{D_{LT}} considering D_{LT} > D_G \quad (11)$$

However, if $D_{LT} \leq D_G$, then $ra = 0$,

where D_G is the depth at the groyne's tip and D_{LT} is the depth of active longshore transport. The latter is given by the formula (Hanson, 1989):

$$D_{LT} = \frac{1.27}{\gamma}\left(H_{s,b)}\right) \quad (12)$$

where γ is the breaking wave index and here was taken equal to *0.78*, while H_{sb} is the significant wave height at breaking position. Eq. (11) is

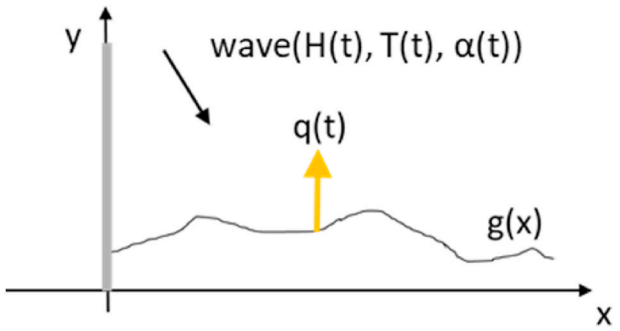

Fig. 4. The grey, vertical bar on the *y* axis symbolizes a groyne; *g(x)* refers to the initial shoreline position, wave time-series of wave height *H(t)*, wave period *T(t)* and wave direction *α(t)* can be incorporated as input-data to the semi-analytical model, as well as a time-varying sediment flow *q(t)* from a source (in case $q > 0$) or sink (in case $q < 0$) of sediment discharge.

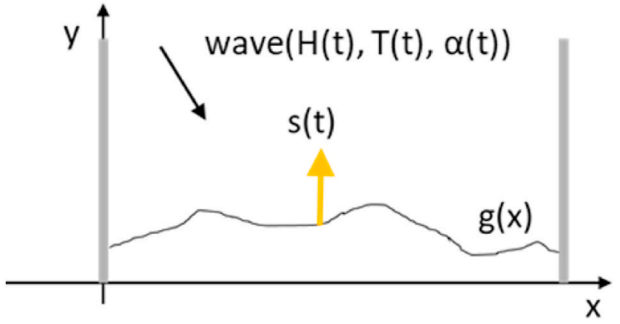

Fig. 5. The two vertical, grey bars denote the two groynes that confine a beach section having initial shoreline position *g(x)*. Apart from a time-varying wave forcing, the groyne compartment might be imposed to a source or sink of sediment material with sediment flow *s(t)*.

postulated on the assumption that the longshore transport is distributed uniformly across the active profile. As Hanson (1989) noted, a thorough analysis of sand transport around groynes would require the cross-shore distribution of the longshore sand transport rate, as well as the 2-d horizontal pattern of sand transport. In the absence of a reliable predictive expression to account for this Eq. (11) is the simplest assumption giving reasonable results. There remains a lack of reliable predictive expressions, verified under prototype conditions, so we have adopted this pragmatic approach here. As is clear from Eq. (12), D_{LT}, the offshore-ward limit of longshore sediment movement, varies in time according to the corresponding significant wave height value in a sequence of wave events. The relationship between D_c and D_{LT} is best considered in terms of time scale. D_c is usually defined in terms of an extreme wave height, corresponding to storm conditions experienced

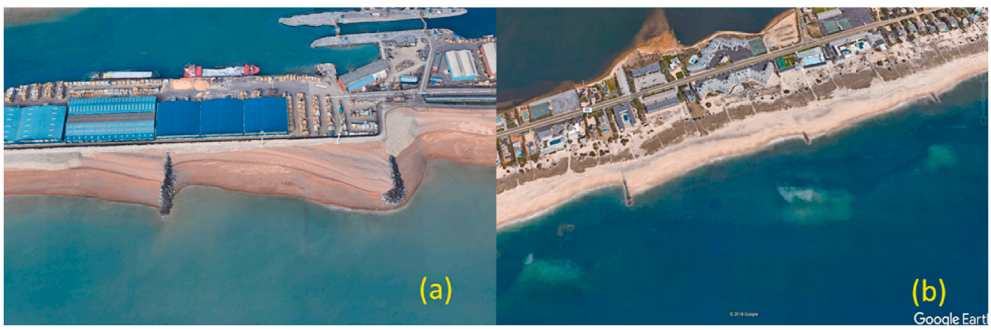

Fig. 3. (a) The terminal groyne syndrome occurring in Southwick beach in West Sussex where the net littoral drift is from left to right. (b) The same phenomenon is observed in Westhampton beach in New York where the net littoral drift is from right to left (photos extracted from Google Earth).

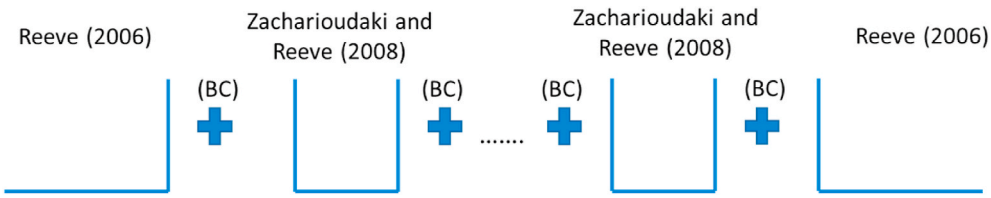

Fig. 6. With the proper internal boundary, the semi-analytical models can be combined to describe a groyne field.

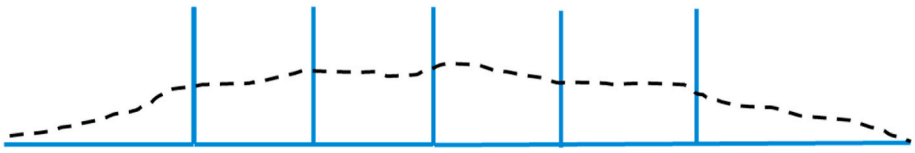

Fig. 7. A groyne field comprising of 5 groynes, and open external boundary conditions. The black intermittent line corresponds to the initial shoreline position.

once every few years. D_{LT} defines the instantaneous value of the seaward extent of the active profile. Under extreme conditions it will equal D_c, but under calmer ones it will be smaller than D_c. The concept of D_c is inextricably linked to wave height, and thus the period over which wave heights are measured to determine their maximum value. A longer period of observation is more likely to include a major storm event in which the cross-shore profile is altered, thus leading to a greater value of D_c. In practice there is a finite limit to the length of records and a pragmatic choice for D_c has to be made. Various authors have suggested formulae, (e.g. Birkemeier 1985), but all are quite close to the formulation of Hallermeier (1983) that gives the annual depth of closure as being approximately twice the annual maximum wave height.

However, as the depth at the groyne tip, D_G, may change in time due to the shoreline movement, and in addition, D_G may be different on the updrift and downdrift side off the groyne, Eq. (11) cannot be applied without taking into consideration a time-varying D_G (Fig. 8):

Consequently, a time-varying water depth $D_G(t)$ is introduced in this study, assuming a constant cross-shore seabed slope *sl* and the horizontal distance between the shoreline position $y(t)$ and the tip of the groyne, where the water-depth $D_G(t)$ is taken into account (Fig. 9). Subsequently, $D_G(t)$ is given by Eq. (13):

$$D_G(t) = sl(y_{GB} + L_G - y(t)) \tag{13}$$

where L_G is the groyne's length measured from the point it intersects the initial shoreline up to the groyne's seaward tip, y_{GB} is the distance from the shore-ward end of the groyne (namely, the point where the initial shoreline intersects the groyne) to the *x*-axis, and $y(t)$ is the shoreline position at time *t*, (Fig. 9). The physical meaning of Eq. (13) is that as the shoreline near the groyne changes in time, the depth $D_G(t)$ is expected to change as well.

The horizontal distance between the shoreline at the groyne and the calculated depth of active longshore transport is denoted by y_{LT}, (Fig. 9). $y_{LT}(t)$ describes the cross-shore zone of active longshore sediment transport. $y_{LT}(t)$ is expected to alter in time as the shoreline evolves, and consequently, the depth of active longshore transport, $D_{LT}(t)$, changes due to the time-varying hydrodynamic forcing (Eq. (12)). Thus, $y_{LT}(t)$ is given via Eq. (14):

$$y_{LT}(t) = \frac{D_{LT}(t)}{sl} \tag{14}$$

Bypassing will occur under the following condition given from Eq. (11), namely $D_{LT}(t) > D_G(t)$. This condition ensures that the active water-depth D_{LT} is greater than the water-depth at the groyne so that sediment bypassing can occur.

Thus, the portion of longshore sediment flux *ra* that bypasses a groyne is given by Eq. (15):

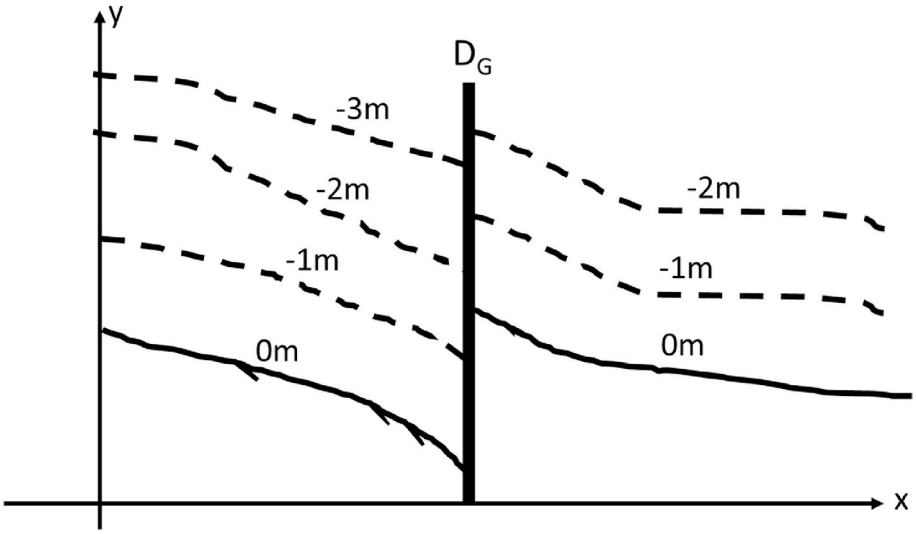

Fig. 8. The morphodynamic evolution on the updrift and downdrift side of a groyne alter the water depth D_G at the tip of the groyne. The solid line corresponds to the shoreline and the intermittent lines to the bathymetric contours.

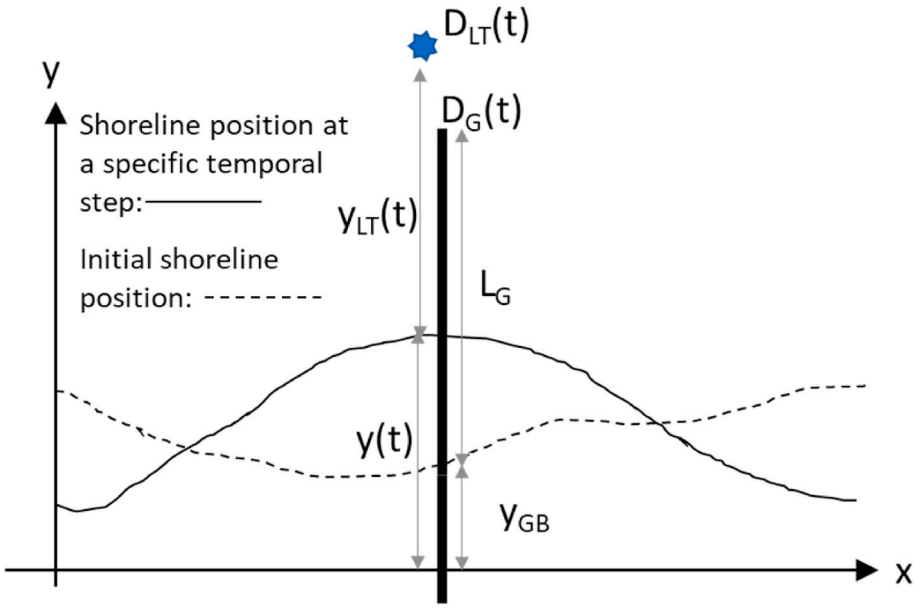

Fig. 9. Schematic illustration of the internal boundary condition introduced in this study.

$$ra = 1 - \frac{L_G - (y(t) - y_{GB})}{y_{LT}(t)} \tag{15}$$

The physical meaning of Eq. (15) is that only the part of the cross-shore beach profile up to the depth of active longshore transport, which is not shadowed by the groyne, contributes to the bypassing process. Therefore, in the case where $y\text{-}y_{GB} = L_G$, in other words, the updrift side of the groyne is full, then, $ra = 1$, and the full amount of sediment flux passes from the updrift side of the groyne to the downdrift, while, if $y_{LT} \leq L_G$ -$(y\text{-}y_{GB})$, namely, the whole zone of active longshore transport y_{LT} is shadowed by the groyne, then, $ra = 0$, and no bypassing takes place.

With the above assumptions, an internal impermeable groyne of finite length may be simulated according to the following boundary condition:

$$\frac{\partial y}{\partial x} = a_0(1 - ra) \tag{16}$$

where $\frac{\partial y}{\partial x}$ is the local gradient of the shoreline curve; and α_0 is the angle of breaking wave crests in relation to the shore normal.

In addition to the possibility of bypassing, sediment material might pass through the body of a groyne such as when it is made of rocks. Hanson (1989) proposed a relation to describe the total amount of sediment movement from the updrift to the downdrift side of the groyne:

$$F = p(1 - ra)\cdot + \cdot ra \tag{17}$$

where F is the portion of the longshore sediment flow which passes to the downdrift side of a groyne; while p is the portion of the longshore sediment transport which corresponds to the permeability of the groyne.

Under the combined effect of sediment bypassing and permeability the internal boundary condition at the groyne is as follows:

$$\frac{\partial y}{\partial x} = a_0(1 - F) \tag{18}$$

It should be noted that the condition described by Eq. (16) embodies a modification of the physics described by the more familiar impermeable condition. The physical meaning of Eq. (16), (and Eq. (18)), can be understood as follows. In the case of an impermeable, infinitely long groyne all sediment transport past the groyne is halted. This is equivalent to the beach plan shape being parallel to the incoming wave crests. This doesn't prevent accumulation of sediment on the updrift beach but fixes the angle of the beach at the groyne. In a computational model based on a staggered grid, the transport rates are calculated at half-points while groynes are placed at whole points. A by-passing formula akin to Eq. (16) can thus be implemented by using the transport rates near but not at the groyne, (Hanson 1989). In an analytical model the boundary condition is implemented at the location of the groyne and a by-passing criterion embedded within it at this point. To represent by-passing the condition of zero transport must be modified. Within the constraints of the 1-line model this require the beach plan shape gradient to be modified so that it is not parallel to the wave crests at the groyne. This was recognised by Larson et al. (1997) who proposed a formula to mimic by-passing based on the fullness of the groyne (i.e. the proportion of the groyne length to which the beach on the updrift side had reached), that also adjusted the beach angle at the groyne.

For small wave angles the sediment transport rate along the shoreline is given by the following formula:

$$Q = Q_0\left(2a_0 - 2\frac{\partial y}{\partial x}\right) \tag{19}$$

where Q_0 is the amplitude of longshore sediment transport rate. The combination of Eqs. (18) and (19) yields Eq. (20) which describes the sediment flow due to bypassing of sediment material around the seaward tip of an impermeable groyne:

$$Q = 2a_0Q_0\ F \tag{20}$$

Following the principle of continuity of mass, the sediment flow on the updrift side of the groyne is the same as on the downdrift side, thus, according to Eq. (21):

$$Q^{up} = Q^{down} \Rightarrow 2a_0Q_0F^{up} = 2a_0Q_0F^{down} \Rightarrow F^{up} = F^{down} \tag{21}$$

Therefore, from Eq. (18), it can be concluded that the boundary conditions on the updrift and the downdrift side of a groyne are the same whether bypassing takes place or not:

$$\left(\frac{\partial y}{\partial x}\right)_{up} = \left(\frac{\partial y}{\partial x}\right)_{down} \tag{22}$$

The semi-analytical solutions of Reeve (2006) and Zacharioudaki and Reeve (2008) may be used with the internal boundary conditions above and so may be used to include a sufficiently general form of boundary condition that encompasses beach evolution within a groyne

field.

3. Evaluation of the analytical solution

To illustrate the type of situations in which the methodology described in Section 2 can be applied solutions for several cases are presented here. Calculations are performed for a period of one year. As test cases we consider two initial beach configurations: a straight, north-facing shorefront whose normal is *0°N*; and a beach with the same orientation but with an initial Gaussian shape, given by the mathematical expression: $y(x,0) = 50e^{-(x-5100)^2/500000}$. This initial condition corresponds to the following curve in the domain $0\ m < x < 10{,}200\ m$ and is shown in Fig. 10.

Fig. 10. The convex initial beach condition.

Two forms of wave conditions have been used. The first is a sequence of weekly wave conditions over the one year period. These were created using the method described in Valsamidis and Reeve (2017) and the full set of conditions is provided in Appendix A. The summary statistics are provided in Table 1.

The second wave condition is a constant one, consisting of the mean values of wave height, period and direction from the weekly sequence. The corresponding values are shown in the second column of Table 1. The longshore sediment transport rate was calculated using the CERC longshore sediment transport formula (CERC, 1984),

$$\varepsilon = \frac{K}{D_C + D_B}\left(\frac{C_{gb}}{8(S_g - 1)(1 - po)}\right){H_{sb}}^2, \tag{23}$$

where K is a dimensionless calibration parameter depending on the special characteristics of the coastal system which is under investigation. Here, we set $K = 0.39$ following the guidance in USACE (1984). D_c is the depth of closure taken equal to $6m$, D_B is the berm height which was set equal to $1m$; C_{gb} is the group velocity of the waves at breaking and s_g is the dimensionless magnitude of the specific gravity assigned the value 2.65; po is the porosity, set to 0.4 which is typical of sandy beaches; and H_{sb} is the significant wave height. Table 2 summarises the different cases for which results are shown.

In the first case, the initially straight beach is identical to the x-axis in a Cartesian system, and the y-axis measures the shoreline position relative to the x-axis, as shown in Fig. 11. This beach extends $10{,}200\ m$ in length and it includes a groyne field consisting of 3 groynes denoted Groyne 1, Groyne 2 and Groyne 3 located at x = 4650 m, 5100 m and 5550 m respectively. Each groyne extends $50\ m$ in the offshore direction from the initial shoreline position, and also extends landward in the negative y-axis direction, to avoid undercutting. The seabed gradient is taken to be 1%. The external boundary conditions are free, allowing sediment material to enter and leave the domain.

Table 1
Statistical characteristics of the wave time-series.

	Range of values	Mean value	Standard deviation
Wave height (Hs)	0 m–1.30 m	0.52 m	0.22 m
Wave Period (T)	1 s–12 s	5.93 s	2.02 s
Wave direction (α)	−0.13 rad–0.19 rad	0.04 rad	0.05 rad

Table 2
Summary of illustrative test cases.

Case No.	Initial condition	Wave condition	Groynes
1	Straight	Constant	Infinite, impermeable
2	Straight	Constant	Impermeable, by-passing
3	Straight	Constant	Permeable, by-passing
4	Gaussian	Constant	Infinite, impermeable
5	Gaussian	Constant	Impermeable, by-passing
6	Gaussian	Constant	Permeable, by-passing
7	Straight	Varying	Impermeable, by-passing
8	Gaussian	Varying	Impermeable, by-passing

Fig. 11. The model was firstly evaluated for constant incident wave conditions that are the mean values of the wave time-series included in Table 1, namely, $Hs = 0.52\ m$; $T = 5.93$ s; and $\alpha = +0.04$ rad.

The first three cases listed in Table 2 correspond to this situation for, respectively: a) infinitely long impermeable groynes; b) sediment bypassing around the seaward tips of impermeable groynes; and c) sediment bypassing around the seaward tips of groynes which are considered to be 20% permeable.

The shoreline positions for these three cases, after 1 year, are shown in Fig. 12.

Fig. 12. The choice of a 1 year period is arbitrary but typical of the periods used for the type of simulation made using 1-line models. Fig. 12 shows the qualitative behaviour that would be anticipated in the three different cases, with by-passing and permeability alleviating the 'terminal groyne syndrome' often encountered on the downdrift edge of groyne systems that interrupt the littoral drift. Fig. 13 shows the time

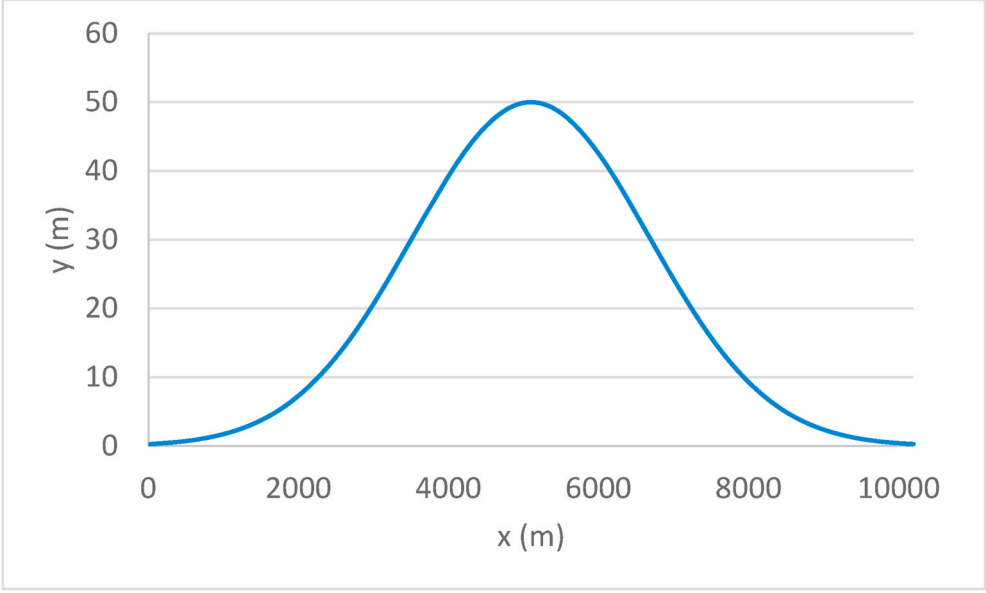

Fig. 10. A Gaussian curve was chosen as an initial condition in the modelling process, alternatively to an initially straight shoreline position.

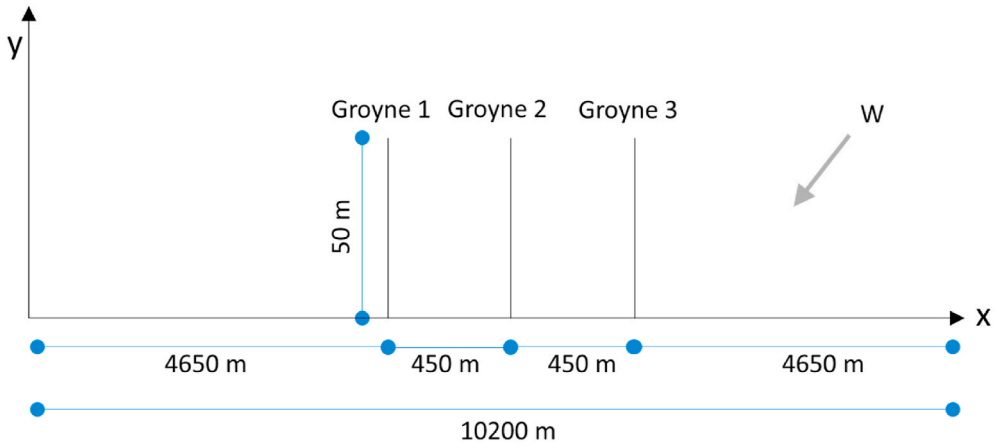

Fig. 11. The modelled area is characterized by free boundary conditions at x = 0 m and x = 10,200 m, and 3 groynes in the middle, obstructing sediment transport along the shore.

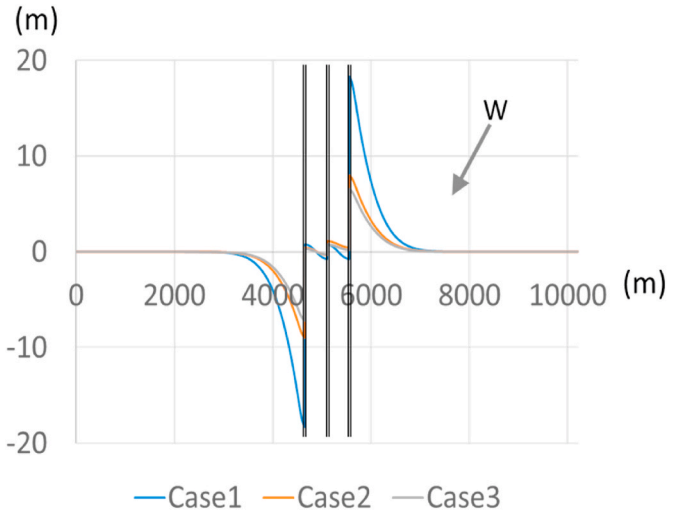

Fig. 12. The double vertical lines symbolize the 3 groynes. Three different scenarios are shown: impermeable groynes with no by-passing (blue); impermeable groynes with by-passing (orange); and permeable groynes with by-passing (grey). (For interpretation of the references to colour in this figure legend, the reader is referred to the Web version of this article.)

history of the transport rate at Groyne 3 over the one year period. This shows low rates initially, due to permeability. After a few weeks accumulation on the updrift side of the groyne is sufficient to activate some by-passing, which continues to increase slightly over the remainder of the period, demonstrating that an equilibrium state has not yet been reached.

Fig. 13. The three groynes divide the domain into four sections, 1 to 4, from left to right. Thus Section 1 is 0 m < x < 4650 m, Section 3 is 5100 m < x < 5550 m and so on. Table 3 summarises the net transport rates within the domain over the 1 year period, by quarter for Case 3. Results are quoted with units of m^2/yr/linear metre and are calculated from the area change in each section, divided by the length of the section and the duration.

For each quarter, summing the products of the quoted rate and the respective lengths of each section yields a value of effectively zero, (to rounding error), confirming the overall conservation of sediment. The rates for the first quarter are slightly below those for the remaining quarters due to inaccuracies in evaluating Eqs. (2) and (4) for very small values of *t*.

The corresponding shoreline positions after 1 year for Cases 4 to 6 are shown in Fig. 14 and the net transport rates in Table 4.

Fig. 14.

In this case the diffusion of the initial hump across the boundaries of the finite domain will result in the net loss of sediment from the domain. The semi-analytical solutions are valid on an infinite domain so the apparent sediment loss arises from performing the calculations on a finite portion of the infinite domain which does not fully contain the disturbance of the beach from a straight line. The initial condition introduces an asymmetry into the problem with outward spreading of the hump is combined with wave-driven transport from left to right in Fig. 14. As a result the transport rates in Section 1 and 4 are not equal and opposite as for the initially straight beach, which results in rapid erosion in the lee of Groyne 1, even with permeable groynes and by-passing occurring.

Finally, the shoreline response after 1 year for Cases 7 and 8, for a randomly varying wave climate described in Table 1, are shown in Fig. 15.

Fig. 15. The instantaneous transport rates at Groyne 3 for Case 8 are plotted in Fig. 16 and illustrate intermittent drift reversal throughout the year. Net transport rates for cases 7 and 8 are presented in Table 5.

Fig. 16.

4. Discussion

Semi-analytical solutions for beach evolution within a groyne field have been presented. The range of situations for which analytical solutions can be derived has been extended to include an extended groyne field in which the initial shoreline shape is not restricted to be straight, the groynes may be permeable and of finite length which allows by-passing. The shoreline response to wave forcing, as predicted by the new semi-analytical solution is in agreement with physical considerations sediment transport and sediment conservation. For instance, in Fig. 12 accretion is observed on the updrift side of the groynes and erosion on the downdrift side. Moreover, depending on the internal boundary condition, namely, absolute blockage of sediment transport; impermeable groyne with sediment by-passing; or permeable groyne with sediment by-passing, the amount of accretion observed on the updrift side of the groynes decreases, respectively, and as a result, the amount of erosion on the downdrift side of the groynes decreases proportionally. Also, in the case where the groynes are permeable or by-passing the start of sequential filling of the groyne compartments is evident, in accordance with the direction of the longshore transport. This process is far from completed and the beach configuration shown in Fig. 12 is not an equilibrium state, as evident from the sediment transport rates, (Fig. 13), which show a continuing but gradual rise after one year.

The case where the beach shape is not a straight line introduced some

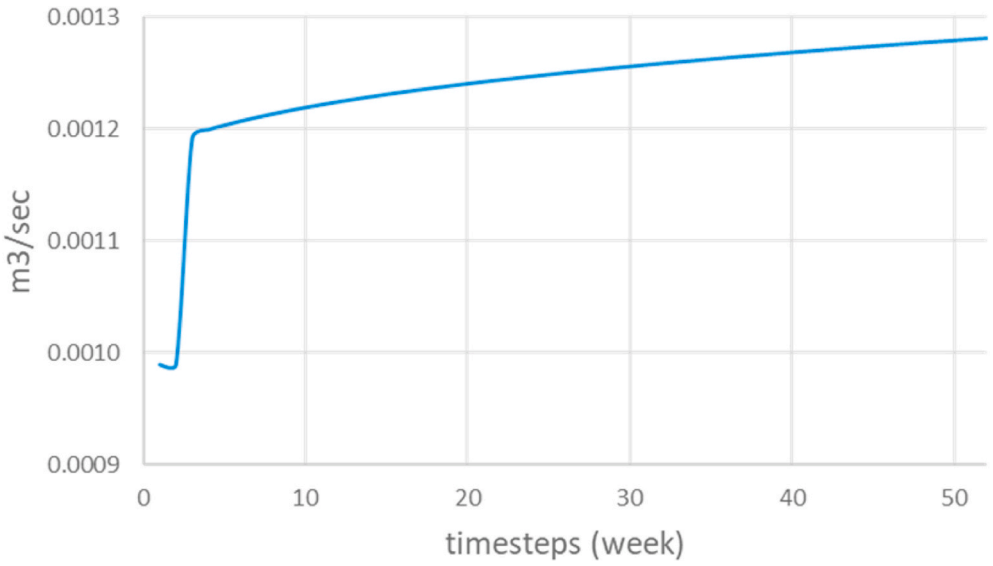

Fig. 13. Time history of the sediment transport rate at Groyne 3 in Case 3.

Table 3
Net transport rates by quarter and section, (m^2/yr/m), for Cases 1 to 3.

Period \ Region	Section 1	Section 2	Section 3	Section 4
Case 1				
1st Quarter	−1.72	0.00	0.00	1.72
2nd Quarter	−1.80	0.00	0.00	1.80
3rd Quarter	−1.80	0.00	0.00	1.80
4th Quarter	−1.80	0.00	0.00	1.80
Case 2				
1st Quarter	−0.75	0.00	0.24	0.72
2nd Quarter	−0.88	0.02	0.73	0.81
3rd Quarter	−0.88	0.06	0.99	0.78
4th Quarter	−0.88	0.10	1.17	0.76
Case 3				
1st Quarter	−0.61	0.00	0.03	0.60
2nd Quarter	−0.71	0.01	0.49	0.66
3rd Quarter	−0.70	0.03	0.66	0.64
4th Quarter	−0.70	0.05	0.79	0.62

interesting features. It may be noticed that in Fig. 14 the amount of accretion on the updrift side of Groynes 3 and 2 with the Gaussian initial shoreline appears smaller than the corresponding amount of accretion for the case of an initially straight shoreline. Further, the magnitude of erosion on the downdrift side of Groyne 1 is larger for Case 1 than Case 2. These observations may be explained by the diffusive behaviour of the One-Line model Eq. (1) which tends to smooth salients formed along the shoreline. Specifically, the peak of a salient retreats over time towards the baseline while at locations on its flanks may experience accretion due to the sideways spreading, (Larson et al., 1987). To amplify this point, Case 1 which is illustrated in Fig. 14 was repeated with the wave direction fixed so that $\alpha = 0$, and the internal boundary conditions set to impermeable groynes of theoretically infinite length. The shoreline will evolve to align itself to the incoming wave crests. The beach in the groyne compartments straightens while the beach outside this area spreads, with the peak retreating fastest and the flanks accreting slightly, as shown in Fig. 15.

Fig. 15.

All results show that there is greater accumulation of sediment material in the first groyne compartment encountered by the predominant longshore drift, namely between Groynes 2 and 3, than in the subsequent groyne compartment, defined by Groynes 1 and 2. This arises from the greater sensitivity of the beach response to the groyne that first intercepts the longshore transport. This phenomenon can be understood physically from the greater mobilization and supply of sediment in an

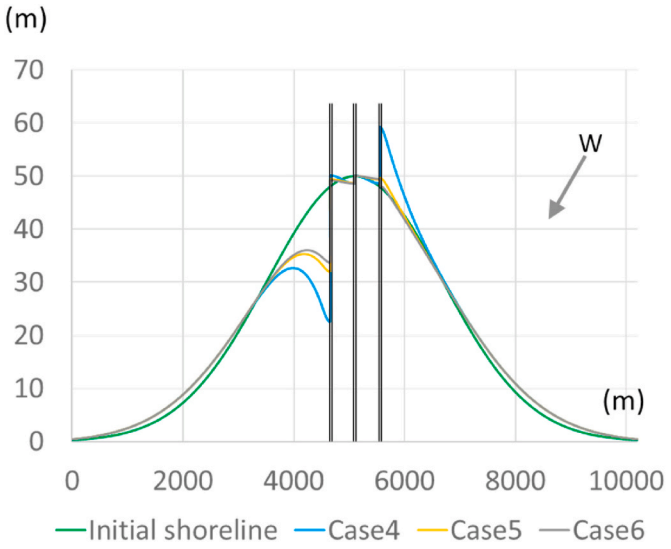

Fig. 14. Shoreline position at the end of 1 year for Cases 4 to 6. The Gaussian-shaped initial shoreline position is depicted with a green line. The double vertical lines symbolize the 3 groynes. Three different cases are shown: impermeable groynes with no by-passing (blue); impermeable groynes with by-passing (orange); and permeable groynes with by-passing (grey). (For interpretation of the references to colour in this figure legend, the reader is referred to the Web version of this article.)

area with an open boundary as opposed to a groyne compartment in which the supply of sediment is more confined. Thus, when sediment material is allowed to pass from the one compartment to another, (for instance Cases 2 and 3 in Fig. 12), more sediment material may be entering the updrift groyne compartment (the area between Groynes 2 and 3) than leaving. In contrast, there is an approximate balance in sediment material entering and exiting the downdrift groyne compartment (between Groynes 1 and 2). This is apparent in Fig. 12 (cases 2 and 3), where the shoreline position is almost the same for all the 3 cases, indicating that there is virtually no net sediment material accumulation or loss. One way to produce an accretion trend in the second groyne compartment (the area between Groynes 1 and 2) would be to decrease the permeability of Groyne 1 to prevent sediment material from exiting this groyne compartment. Thus, Case 3 which is illustrated in Fig. 12,

Table 4
Net transport rates by quarter and section, (m^2/yr/m), for Cases 4 to 6.

Period \ Region	Section 1	Section 2	Section 3	Section 4
Case 4				
1st Quarter	−1.57	0.00	0.00	1.44
2nd Quarter	−1.84	0.00	0.00	1.76
3rd Quarter	−1.84	0.00	0.00	1.76
4th Quarter	−1.84	0.00	0.00	1.76
Case 5				
1st Quarter	−0.84	−0.22	0.70	0.66
2nd Quarter	−0.89	−0.31	0.20	0.83
3rd Quarter	−0.90	−0.29	0.26	0.82
4th Quarter	−0.90	−0.27	0.28	0.82
Case 6				
1st Quarter	−0.71	−1.16	1.24	0.57
2nd Quarter	−0.73	−0.40	0.24	0.67
3rd Quarter	−0.73	−0.18	0.03	0.67
4th Quarter	−0.73	−0.17	0.02	0.66

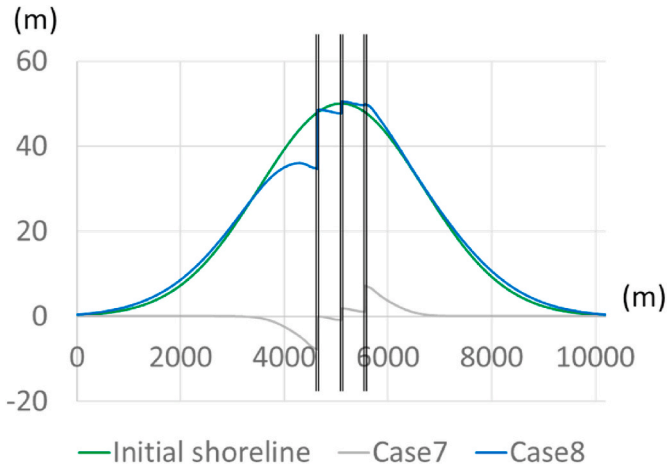

Fig. 15. Shoreline positions after 1 year for Cases 7 and 8. The wave conditions are described in Table 1, and the internal boundary conditions correspond to permeable groynes allowing bypassing.

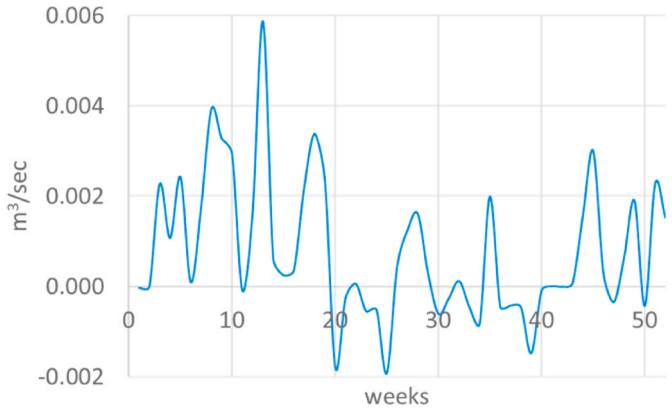

Fig. 16. The instantaneous transport rates at Groyne 3 for Case 8.

was slightly altered considering the permeability to be $p = 0$ at Groyne 1. The resulting calculation produced the complementary Case 3* which is plotted versus Case 3 in Fig. 16.

Fig. 16 shows that if Groyne 1 is impermeable then accretion occurs on its updrift side, however, the terminal groyne effect (Fig. 3) is exacerbated on the downdrift side.

The concept of varying the permeability of groynes is being implemented in a new generation of groynes which can be adjusted to the prevailing morphodynamic conditions (e.g. MENA Report, 2014). An example is shown in Fig. 17. This type of structure will have a permeability that varies with beach position, and therefore with time (see Fig. 19) (see Fig. 18).

Table 5
Net transport rates by quarter and section, (m^2/yr/m), for Cases 7 and 8.

Period \ Region	Section 1	Section 2	Section 3	Section 4
Case 7				
1st Quarter	−1.83	0.00	1.38	1.70
2nd Quarter	−1.26	−0.93	2.92	1.03
3rd Quarter	−0.15	−0.87	0.74	0.19
4th Quarter	−0.26	−0.25	0.60	0.25
Case 8				
1st Quarter	−1.83	−0.62	0.87	1.68
2nd Quarter	−1.23	−1.78	2.11	1.10
3rd Quarter	−0.11	−1.54	−0.04	0.25
4th Quarter	−0.24	−0.81	−0.10	0.29

Fig. 17.Just such behaviour can be incorporated directly into the new semi-analytical solution through the time varying internal boundary conditions. (In this regard it is worth noting that the sediment movement through a permeable groyne is activated in the modelling process only when $y(t)\text{-}y_{GB}(t) > 0$.)

Finally, a comparison between the beach response to constant wave conditions and varying wave conditions, (comparing Figs. 11 and 14 with Fig. 15), shows that including for the occurrence of temporary drift-reversal ameliorates the beach response.

5. Conclusions

One limitation of analytical solutions has been their applicability solely to simple situations such as a single groyne or single groyne compartment. In this paper we have proposed a means of accounting for sediment transmission through permeable groynes and by-passing groynes of finite length under time varying wave conditions. The underlying concept is based on the concept of the instantaneous active depth of longshore transport introduced by Hanson (1989) for computational modelling; modified to account explicitly for non-zero transport at the groyne by adjusting the gradient of the beach planshape at the groyne according to the extent of the active depth beyond the groyne tip. This has provided an analytical means of calculating the beach plan shape evolution in a groyne field consisting of an arbitrary number of groynes, which represents a considerable increase in the complexity of beach configurations amenable to analytical treatment.

The internal boundary conditions have been combined with the solutions for shoreline evolution near a groyne (Reeve, 2006) and

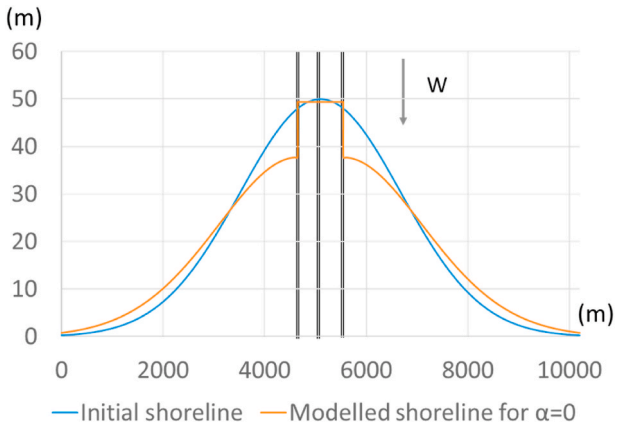

Fig. 17. Shoreline evolution after 1 year of an initially Gaussian shaped shoreline, for wave direction $\alpha = 0$ and impermeable groynes, (denoted with double vertical lines).

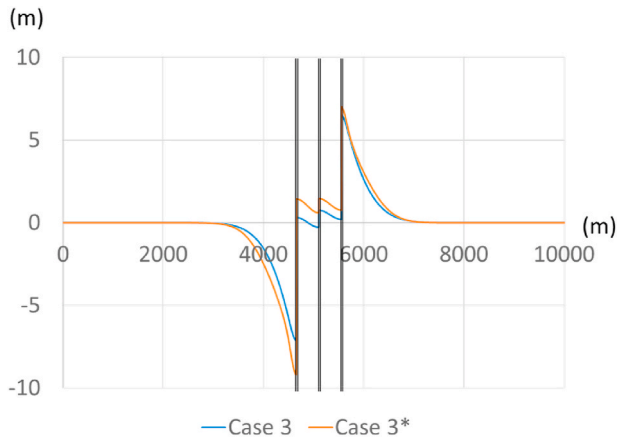

Fig. 18. Case 3* is the same as Case 3 except for the fact that Groyne 1 is impermeable.

Fig. 19. The innovative groyne design concept that allows for adjustment of groyne permeability by adding/removing pre-cast concrete blocks (photo: Cortez beach, Florida).

shoreline evolution in a groyne compartment (Zacharioudaki and Reeve, 2008). A range of solutions have been presented to illustrate the type of situations that may be modelled. These are all based on a one year period with a groyne field comprising three groynes in which the groynes were impermeable and of infinite length; impermeable and of finite length, permitting sediment bypassing; permeable and of finite length permitting bypassing. Two initial beach conditions were also considered: a straight shoreline and a Gaussian-shaped curve that mimicked a large nourishment or ness. Two forms of wave condition were considered: constant, as commonly assumed in early analytical solutions; and time-varying on a weekly basis.

The solutions capture the qualitative beach behaviour observed in practice. Quantitative results have also been provided, expressed as instantaneous and net transport rates. The different internal boundary conditions mimic the effect of impermeable and permeable groynes, as well as by-passing. The description of these processes is a simplified version of reality that is consistent with the 1-line concept. One caveat of the method is that it can be difficult to evaluate for very small time periods; in the cases studied here this equated to periods of a week or less. However, as the 1-line concept is applied to problems simulating periods of months to years this is not seen as a major impediment. The methodology proposed in this paper also provides the means to develop new analytical solutions of more complicated situations for testing computational models.

Declaration of competing interest

The authors declare that they have no known competing financial interests or personal relationships that could have appeared to influence the work reported in this paper.

Acknowledgements

The support of the UK Engineering and Physical Sciences Research Council (EPSRC) under the MORPHINE project (grant EP/N007379/1) is gratefully acknowledged.

Appendix A. Wave time series used as input-data to the semi-analytical solution

Wave Height (m)	Wave Period (sec)	Wave Direction (rad)
0.39	3.5	0.04
0.20	2.3	−0.09
0.55	3.4	0.01
0.98	5.1	0.17
0.42	4.8	0.19
0.12	2.2	−0.14
0.46	3.1	0.10
0.73	3.9	0.07
0.96	4.9	0.16
0.67	4.0	0.16
1.08	5.1	0.18
0.66	3.8	0.22
0.61	4.4	0.01
0.35	4.3	0.17
0.74	3.9	−0.09
0.37	3.4	−0.04
0.17	2.6	−0.03
0.76	4.0	0.24
0.57	4.3	0.13
0.73	3.8	0.28

(continued on next page)

(*continued*)

Wave Height (m)	Wave Period (sec)	Wave Direction (rad)
0.29	2.7	0.18
0.59	3.8	0.14
0.82	4.6	0.17
0.57	3.6	0.08
0.66	3.6	0.13
0.83	4.2	0.18
0.86	4.7	0.07
1.08	5.4	0.03
0.96	4.8	0.16
1.11	5.6	0.17
0.88	4.6	0.04
1.00	5.4	−0.02
1.10	5.2	0.04
1.02	5.1	0.12
1.22	6.4	0.21
0.98	5.2	0.18
1.04	5.7	0.04
0.33	1.8	0.09
0.42	2.8	0.04
0.96	5.2	0.16
0.25	1.3	−0.02
0.22	2.3	0.05
0.93	4.8	0.13
0.92	5.1	0.18
1.04	6.0	0.12
0.57	4.6	0.11
0.58	4.1	−0.09
0.42	2.6	−0.03
0.79	4.4	0.16
0.93	5.1	0.12
0.42	2.7	0.06
0.76	4.5	0.09

References

Bakker, W.T., 1969. The Dynamics of a Coast with a Groyne System. Proc 11th Coastal Engrg Conf, pp. 492–517. ASCE, New York, N.Y.

Basco, D.R., Pope, J., 2004. Functioning and design of coastal groins: the interaction of groins and the beach—process and planning. Journal of Coastal Research, v. WINTER 121–130.

Birkemeier, W.A., 1985. Field data on seaward limit of profile change. Journal of Waterway, Port, Coastal and Ocean Engineering, ASCE 111 (3), p598–602.

CERC, 1984. Shore Protection Manual: Vicksburg, Coastal Engineering Research Center. U. S., Corps of Engineers.

Clarke, J., Milburn, C., Stevens, A., Townsend, D., Dowsett, H., Thomas, R., 2017. Regional Beach Management Plan 2017: Littlehampton to Brighton Marina: Canterbury. Environment Agency.

Coghlan, I., Carley, J., Cox, R., Davey, E., Blacka, M., Lofthouse, J., 2013. Concept Designs for a Groyne Field on the Far North SSW Coast: 22nd NSW Coastal Conference. Port Macquarie, New South Wales.

Fleming, C.A., 1990. Guide on the Use of Groynes in Coastal Engineering, vol. 119. CIRIA Report, London, UK.

Gravens, M.B., Kraus, N.C., Hanson, H., 1991. GENESIS: Generalized Model for Simulating Shoreline Change: Report 2, Workbook and System User's Manual. U. S. Army Corps of Engineers.

Hallermeier, R.J., 1983. Sand Transport Limits in Coastal Structure Design. Proc. Coastal Struct., 1983, ASCE, pp.703–716.

Hanson, H., 1987. GENESIS-A Generalized Shoreline Change Numerical Model for Engineering Use. Lund Inst. of Tech/.Univ. of Lund, Lund.

Hanson, H., 1989. Genesis: a generalized shoreline change numerical model. J. Coast Res. v. 5, 1–27.

Hanson, H., Kraus, N.C., 1989. Genesis: generalized model for simulating shoreline change. Tech. Report. In: CERC-, vols. 89–19. USACE, Washington, DC, 247pp.

Hanson, H., Bocamazo, L., Larson, M., Kraus, N.C., 2008. Long-term Beach Response to Groin Shortening, Westhampton Beach, Long Island. International Conference on Coastal Engineering: Hamburg, Germany, ASCE, New York, pp. 1927–1939.

Horikawa, K., Harikai, S., Kraus, N.C., 1979. A Physical and Numerical Modelling of Waves, Current and Sediment Transport Near a Breakwater, vol. 38. Annual Reprot of the Engineering Research Institute, University of Tokyo, pp. pp41–48.

Kraus, N.C., Hanson, H., Blomgren, S.H., 1994. Modern Functional Design of Groin Systems. Coastal Engineering Kobe, Japan.

Larson, M., Hanson, H., Kraus, N.C., 1987. Analytical Solutions of the One-Line Model of Shoreline Change: Technical Report CERC-87-15, USAE-WES. Coastal Engineering Research Center, Vicksburg, Mississippi.

Larson, M., Hanson, H., Kraus, N.C., 1997. Analytical solutions of one-line model for shoreline change near coastal structures. J. Waterw. Port, Coast. Ocean Eng. v. 123, 180–191.

Mena, Report, 2014. Cortez Groins Removal and Replacement Project: Tender Documents: T24356360. Albawaba (London) Ltd.

Pelnard-Considère, R., 1956. Essai de théorie de l'évolution des formes de rivage en plages de sables et de gâlets: Societe Hydrotechnique de France, IV'ème Journees de L'Hydraulique Question III, vol. 1, 74-1-10 rapport.

Perlin, M., Dean, R.G., 1979. Prediction of beach planforms with littoral controls. Proc Coastal Structures '79, pp792–808. ASCE.

Perlin, M., Dean, R.G., 1983. A Numerical Model to Simulate Sediment Transport in the Vicinity of Structures, Report, MR-, 83-10.

Reeve, D.E., Valsamidis, A., 2014. On the stability of a class of shoreline planform models. Coast Eng. v. 91, 76–83.

Shibutani, Y., Kuroiwa, M., Matsubara, Y., Kim, M., Abualtaef, M., 2009. Development of N-line numerical model considering the effects of beach nourishment. J. Coastal Res. SI 56 554–558.

Steetzel, H.J., De vroeg, H., Van Rijn, L.C., Stam, J.L., 1988. Morphological Modelling Using a Modied Multi-Layer Approach: International Conference on Coastal Engineering, pp. 1927–1939. Copenhagen, Denmark.

US Army Corps of Engineers.Reeve, D.E, 2006. Explicit expression for beach response to non-stationary forcing near a groyne. J. Waterw. Port, Coast. Ocean Eng. v. 132, 125–132.

USACE, 2002. Coastal Engineering Manual (CEM): Washington, DC 20314-1000. U.S. Army Corps of Engineers.

Valsamidis, A., 2016. A Comparative Study of New Beach Modelling Techniques. PhD Thesis. College of Engineering/Swansea University, Swansea, p. 147.

Valsamidis, A., Cai, Y., Reeve, D.E., 2013. Modelling beach-structure interaction using a Heaviside technique: application and validation. J. Coast Res. 410–415.

Valsamidis, A., Reeve, D.E., 2017. Modelling Shoreline Evolution in the Vicinity of a Groyne and a River: Continental Shelf Research, vol. 132, pp. 49–57.

Walton, T.L., 1994. Shoreline solution for tapered beach fill, J wtrwy, port, coast., and oc. Engrg, ASCE 120 (6), 651–655.

Walton Jr., T.L., Dean, R.G., 2011. Shoreline change at an infinite jetty for wave time series. Continent. Shelf Res. v. 31, 1474–1480.

Wind, H.G., 1990. Influence Functions. Proc. 21st Intl. Conf. Coastal Engrg, ASCE. Costa-del-Sol, Malaga, Spain, pp. 3281–3294.

Zacharioudaki, A., Reeve, D.E., 2008. Semianalytical solutions of shoreline response to time-varying wave conditions. J. Waterw. Port, Coast. Ocean Eng. v. 134, 265–274.